

Self-Similar Hot Accretion Flow onto a Neutron Star

Mikhail V. Medvedev¹ and Ramesh Narayan

Harvard-Smithsonian Center for Astrophysics, 60 Garden Street, Cambridge, MA 02138

ABSTRACT

We consider hot, two-temperature, viscous accretion onto a rotating, unmagnetized neutron star. We assume Coulomb coupling between the protons and electrons, and free-free cooling from the electrons. We show that the accretion flow has an extended settling region which can be described by means of two analytical self-similar solutions: a two-temperature solution which is valid in an inner zone, $r \lesssim 10^{2.5}$, where r is the radius in Schwarzschild units; and a one-temperature solution which is valid in an outer zone, $r \gtrsim 10^{2.5}$. In both zones the density varies as $\rho \propto r^{-2}$ and the angular velocity as $\Omega \propto r^{-3/2}$. We solve the flow equations numerically and confirm that the analytical solutions are accurate.

Except for the radial velocity, all gas properties in the self-similar settling zone, such as density, angular velocity, temperature, luminosity, angular momentum flux, are independent of the mass accretion rate; these quantities do depend sensitively on the spin of the neutron star. The angular momentum flux is outward under most conditions; therefore, the central star is nearly always spun-down. The luminosity of the settling zone arises from the rotational energy that is released as the star is braked by viscosity, and the contribution from gravity is small; hence the radiative efficiency, $\eta = L_{acc}/\dot{M}c^2$, is arbitrarily large at low \dot{M} . For reasonable values of the gas adiabatic index γ , the Bernoulli parameter is negative; therefore, in the absence of dynamically important magnetic fields, a strong outflow or wind is not expected. The flow is convectively stable, but may be thermally unstable. The described solution is not advection-dominated; however, when the spin of the star is small enough, it transforms smoothly to an advection-dominated branch of solution.

Subject headings: accretion, accretion disks — stars: neutron

1. Introduction

At mass accretion rates less than a few per cent of the Eddington rate, black holes (BHs) are believed to accrete via a hot, two-temperature, radiatively inefficient, quasi-spherical, advection-

¹Presently at the Canadian Institute for Theoretical Astrophysics, University of Toronto, 60 St. George Street, Toronto, ON, M6P 4B1, Canada; medvedev@cita.utoronto.ca; <http://www.cita.utoronto.ca/~medvedev>; Also at the Institute for Nuclear Fusion, RRC “Kurchatov Institute”, Moscow 123182, Russia

dominated accretion flow, or ADAF (Ichimaru 1977; Narayan & Yi 1994, 1995a,b; Abramowicz et al. 1995; Chen et al. 1995). The physical properties of ADAFs around BHs have been investigated by a number of authors, and detailed spectral models have been applied to observations of BH candidates (see Narayan, Mahadevan & Quataert 1998 and Kato, Fukue & Mineshige 1998 for reviews).

At low mass accretion rates, accretion onto a neutron star (NS) is also expected to occur via a hot, two-temperature flow (Narayan & Yi 1995b; Yi et al. 1996), but the properties of such flows have not been investigated. NS flows are expected to differ from BH ADAFs in several respects. (i) Whereas in the case of a BH the accreting material flows freely and supersonically through the absorbing boundary at the event horizon, in the case of a NS the radial velocity of the material must decelerate to zero. (ii) The accreting material is expected to apply a spin-up or spin-down torque on the NS. Popham & Narayan (1991) and Paczyński (1991) investigated the nature of the torque for a cold thin disk, but the case of a hot flow has not been studied. (iii) For similar mass accretion rates (in Eddington units), the luminosity of a NS accreting via an ADAF is likely to be much higher than that of a BH because a NS has a surface while a BH has an event horizon (Narayan & Yi 1995b; Narayan, Garcia & McClintock 1997; Menou et al. 1999). (iv) The spectra are expected to be different.

We discuss in this paper the structure of a hot accretion flow around a NS, or any other relativistic star with a surface. The flow under consideration is global and extends radially to very large distances (at least thousands of NS radii or more) where it matches onto appropriate outer boundary conditions. We do not attempt a detailed analysis of the boundary layer region near the NS, where the accretion flow meets the star. We present only an approximate analysis of this region, which extends at most a few NS radii above the stellar surface (for a more detailed discussion of the physics of the boundary layer see Popham & Narayan 1991; Paczyński 1991; Titarchuk, Lapidus, & Muslimov 1998; Titarchuk & Osherovich 1999).

The paper is organized as follows. We show in §2 that there is a radially extended region around the NS where the flow “settles” with a radial velocity much less than the local free-fall velocity. We obtain a self-similar solution for this settling region and show that, surprisingly, the density and temperature of this zone are independent of the mass accretion rate. In §3, we discuss physical properties of the accretion flow. In §4 we compare the analytical results with numerical computations and in §5 we discuss the relationship between the settling flow and an ADAF. We conclude with a discussion in §6.

2. Self-Similar Settling Solution

We consider a steady, rotating, axisymmetric, quasi-spherical, two-temperature accretion flow onto a star with a surface. We use the height-integrated form of the viscous hydrodynamic equations

(Ichimaru 1977; Abramowicz et al. 1988; Paczyński 1991; Narayan & Yi 1994):

$$\dot{M} = 4\pi R^2 \rho v, \quad (1)$$

$$v \frac{dv}{dR} = (\Omega^2 - \Omega_K^2) R - \frac{1}{\rho} \frac{d}{dR} (\rho c_s^2), \quad (2)$$

$$4\pi\alpha \frac{\rho c_s^2 R^4}{\Omega_K} \frac{d\Omega}{dR} = \dot{J} - \dot{M} \Omega R^2, \quad (3)$$

$$\rho v T_p \frac{ds_p}{dR} = \frac{\rho v c^2}{(\gamma_p - 1)} \frac{d\theta_p}{dR} - v c^2 \theta_p \frac{d\rho}{dR} = (1 - \delta) q^+ - q_{\text{Coul}}, \quad (4)$$

$$\rho_e v T_e \frac{ds_e}{dR} = \frac{\rho_e v c^2}{(\gamma_e - 1)} \frac{d\theta_e}{dR} - v c^2 \theta_e \frac{d\rho_e}{dR} = \delta q^+ + q_{\text{Coul}} - q^-, \quad (5)$$

where \dot{M} is the mass accretion rate, R is the spherical radius, ρ is the mass density of the accreting gas, v is the radial infall velocity, Ω is the angular velocity, $\Omega_K(R) = (GM/R^3)^{1/2}$ is the Keplerian angular velocity, $c_s^2 = c^2(\theta_p + \theta_e m_e/m_p)$ is the square of the isothermal sound speed, $T_{p,e}$ are the temperatures of protons and electrons, $\theta_{p,e} = k_B T_{p,e}/m_{p,e} c^2$ are the corresponding dimensionless temperatures, α is the Shakura-Sunyaev viscosity parameter, \dot{J} is the rate of accretion of angular momentum, s_p and s_e are the specific entropies of the proton and electron fluids, $\rho_e \simeq (m_e/m_p)\rho$ is the mass density of the electron fluid, γ_p and γ_e are the adiabatic indices of protons and electrons (which, in general, may be functions of T_p and T_e), and q^+ , q^- , and q_{Coul} are the viscous heating rate, radiative cooling rate, and energy transfer rate from protons to electrons via Coulomb collisions, per unit mass. We have assumed that a fraction δ of the viscous heat goes into electrons and a fraction $1 - \delta$ into protons; it is usually assumed in ADAF models that $\delta \ll 1$, but our analysis is general for any value of δ between 0 and 1. Equations (1)–(5) describe the conservation of mass, radial momentum, angular momentum, proton energy and electron energy, respectively.

For simplicity, we have assumed in equation (1) that the flow is spherical. A more accurate treatment would replace R^2 with RH , where the scale height $H = c_s/\Omega_k$. This would introduce minor differences in some of the quantitative results.

In the case of accretion onto a NS we expect the flow to slow down as it settles on the stellar surface, and we expect the density in this settling zone to be significantly higher than for a BH. The increased density would cause more efficient transfer of energy from protons to electrons via Coulomb collisions and more efficient radiation from the electrons. As we show below, this leads to a flow in which q^+ , q^- and q_{Coul} are all of the same order, which is very different from the case of a BH ADAF, where $q^+ \gg q^-, q_{\text{Coul}}$. Another feature of the settling zone, again the result of the large density, is that optically thin bremsstrahlung cooling (which is sensitive to ρ) dominates over self-absorbed synchrotron cooling. We therefore neglect synchrotron emission in our analysis. For simplicity, we neglect also thermal conduction. Comptonization is important over part of the settling zone. However, we have not been able to derive useful analytical results with both bremsstrahlung and Comptonization included. Therefore, we neglect Comptonization in this section, and discuss its effects in §3.3.

The set of equations (1)–(5) must satisfy certain boundary conditions at the neutron star. First, as the flow approaches the surface of the star at $R = R_{NS}$, the radial velocity must become very much smaller than the local free-fall velocity. Second, the angular velocity must approach the angular velocity of the star Ω_{NS} . We use the dimensionless parameter

$$s \equiv \frac{\Omega_{NS}}{\Omega_K(R_{NS})} \quad (6)$$

to represent the spin of the NS.

The radius of the star, and its spin, are the two principal boundary conditions applied at the inner edge of the accretion flow. We assume that the star is unmagnetized, so there are no magnetospheric effects to consider. Two outer boundary conditions, namely the temperature and angular velocity of the gas, are determined by the properties of the gas as it is introduced into the accretion flow on the outside (e.g. from an ambient medium or from a different type of accretion flow such as a thin disk). These outer boundary conditions have little effect on the interior of the flow (see §5 of this paper, and Narayan, Kato & Honma 1997; but see also Yuan 1999). An additional important boundary condition is the mass accretion rate \dot{M} , which is determined by external conditions and which we take to be constant.

2.1. Inner Settling Solution

We consider first the inner region of the flow, $R_{NS} \lesssim R \lesssim 10^{2.5} R_S$, where $R_S = 2GM/c^2$ is the Schwarzschild radius. In this region we expect a two-temperature plasma, with $T_p > T_e$, in which the electrons are relativistic and the protons are non-relativistic: $\theta_e \gg 1$, $\theta_p \ll 1$. The viscous heating rate of the gas, the energy transfer rate from the protons to the electrons via Coulomb collisions, and the cooling rate of the electrons via bremsstrahlung emission are given by

$$q^+ = \alpha \frac{\rho c_s^2 R^2}{\Omega_K} \left(\frac{d\Omega}{dR} \right)^2, \quad (7)$$

$$q_{\text{Coul}} = Q_{\text{Coul}} \rho^2 \frac{\theta_p}{\theta_e}, \quad Q_{\text{Coul}} = 4\pi r_e^2 \ln \Lambda \frac{m_e c^3}{m_p^2}, \quad (8)$$

$$q^- = Q_{\text{ff,R}} \rho^2 \theta_e, \quad Q_{\text{ff,R}} = 48\alpha_f r_e^2 \frac{m_e c^3}{m_p^2}, \quad (9)$$

where α_f is the fine structure constant, r_e is the classical electron radius, $\ln \Lambda \simeq 20$ is the Coulomb logarithm, $c_s^2 \simeq c^2 \theta_p$, and we have neglected logarithmic corrections to the relativistic free-free emissivity. The subscript ‘‘R’’ in $Q_{\text{ff,R}}$ denotes relativistic bremsstrahlung.

We now make a number of simplifications in equations (1)–(5). First, we neglect the radial velocity term vdv/dR in equation (2). Second, we assume that \dot{J} dominates over $\dot{M}\Omega R^2$ on the right-hand-side of equation (3) and we neglect the latter term. Third, we neglect the entropy terms in equations (4), (5); that is, we assume that the heating, cooling and energy transfer terms in

these equations dominate over the entropy gradient terms. All of these assumptions are justified *a posteriori* below. The equations then read

$$\dot{M} = 4\pi R^2 \rho v, \quad (10)$$

$$(\Omega^2 - \Omega_K^2) R = \frac{1}{\rho} \frac{d}{dR} (\rho c_s^2), \quad (11)$$

$$4\pi\alpha \frac{\rho c_s^2 R^4}{\Omega_K} \frac{d\Omega}{dR} = \dot{J}, \quad (12)$$

$$(1 - \delta)q^+ = q_{\text{Coul}} = q^- - q^+\delta, \quad (13)$$

where q^+ , q_{Coul} , and q^- are given by equations (7)–(9).

It is straightforward to show that the simplified equations (10)–(13) have the following self-similar solution,

$$\begin{aligned} \rho &= \rho_0 r^{-2}, & \theta_p &= \theta_{p0} r^{-1}, & \theta_e &= \theta_{e0} r^{-1/2}, \\ \Omega &= \Omega_0 r^{-3/2}, & v &= v_0 r^0, \end{aligned} \quad (14)$$

where $r = R/R_S$ is a dimensionless radius. The normalization coefficients are uniquely related to each other as follows

$$\theta_{p0} = \frac{1}{6} (1 - s^2), \quad (15a)$$

$$\theta_{e0} = \left(\frac{Q_{\text{Coul}}}{Q_{\text{ff,R}}} \frac{\theta_{p0}}{(1 - \delta)} \right)^{1/2} = \left(\frac{\pi \ln \Lambda}{12\alpha_f} \frac{\theta_{p0}}{(1 - \delta)} \right)^{1/2} \simeq 10.9 \left(\frac{1 - s^2}{1 - \delta} \right)^{1/2}, \quad (15b)$$

$$\Omega_0 = \Omega_{K0} s \simeq 7.19 \times 10^4 m^{-1} s \text{ rad/s}, \quad (15c)$$

$$\rho_0 = \frac{9c^2 \Omega_{k0}}{4Q_{\text{Coul}}} \alpha (1 - \delta) \theta_{e0} s^2 \simeq 8.10 \times 10^{-4} m^{-1} \alpha (1 - \delta) \theta_{e0} s^2 \text{ g/cm}^3, \quad (15d)$$

$$v_0 = \frac{\dot{M}}{4\pi R_S^2 \rho_0}, \quad (15e)$$

$$\dot{J} = -6\pi\alpha c^2 R_S^3 \rho_0 \theta_{p0} s = -\frac{9\pi}{2\sqrt{3}} \frac{(GM)^2 c}{\sqrt{Q_{\text{Coul}} Q_{\text{ff,R}}}} \alpha^2 (1 - \delta)^{1/2} s^3 (1 - s^2)^{3/2}. \quad (15f)$$

Here, $\Omega_{K0} = \Omega_K(R_S)$ and the dimensionless spin parameter is $s = \Omega(R_S)/\Omega_{K0} = \Omega_{NS}/\Omega_K(R_{NS}) = \Omega(R)/\Omega_K(R)$, as introduced in equation (6). Recall that s is a boundary condition of the problem.

The range of r over which the solution is valid is determined by the twin requirements that the protons be non-relativistic and that the electrons be relativistic. The former condition is satisfied for any $r > 1$, while the latter condition requires $r < \theta_{e0}^2 \simeq 120$. A third condition is that Comptonization should be negligible (since we have assumed this). As we show in §3.3, this last condition requires $r > \text{few tens}$, with the exact limit depending on the NS spin, s , and viscosity, α .

The radial velocity of the solution is independent of r , whereas the local free-fall velocity varies as $v_{ff} = c/\sqrt{2r}$. Thus, v/v_{ff} decreases with decreasing radius. This shows that the solution

corresponds to a settling flow and that it is quite different from self-similar ADAFs around BHs, where v/v_{ff} either is constant (Narayan & Yi 1994, 1995a; Manmoto et al. 2000) or increases with decreasing r (Narayan et al. 2000; Quataert & Gruzinov 2000). Although v/v_{ff} is quite small as the flow approaches the NS surface, v itself is still fairly large. At the NS surface, v must reduce substantially from its self-similar value. As the numerical results of §4 show, this happens in a boundary layer where the accreting material cools catastrophically to a temperature that is orders of magnitude below virial. The boundary layer is distinct from the settling zone which is described by the above self-similar solution.

The angular velocity of the gas is a fixed fraction of the local Keplerian angular velocity, the ratio being determined by the dimensionless spin s of the star. The gas in the settling solution radiates most of the energy dissipated through viscosity. In fact, the rates of viscous heating, Coulomb energy transfer and radiative emission are all equal, which is achieved by a suitable choice of the density, electron temperature and proton temperature in the gas. The two temperatures have universal forms, with only a weak dependence on s , while the density has a strong dependence on s .

The most outstanding feature of the self-similar solution is that, except for the radial velocity, none of the other gas parameters has any dependence on \dot{M} .

The fact that \dot{J} is negative implies that the accretion flow removes angular momentum from the star and spins it down. This behavior is quite different from that seen in thin disks (Popham & Narayan 1991; Paczyński 1991), where for most choices of the stellar spin parameter s , the accretion disk spins up the star with a torque $\dot{J}_{\text{thin}} \approx \dot{M}\Omega_K(R_{NS})R_{NS}^2$. Only when s is very close to unity does the torque become negative. In contrast, for the self-similar solution derived here, the torque is negative for all values of s (except extremely small values, see the discussion in §4). Moreover, \dot{J} is independent of \dot{M} . Equivalently, the dimensionless torque, $j = \dot{J}/\dot{M}\Omega_K(R_{NS})R_{NS}^2$, which is ~ 1 under most conditions for a thin disk, here takes on the value

$$\begin{aligned} j &= -\frac{\sqrt{\pi}}{8\sqrt{2}} \frac{m_p}{m_e} \frac{\eta}{\sqrt{\alpha_f \ln \Lambda}} r_{NS}^{-1/2} (1-\delta)^{1/2} \alpha^2 \dot{m}^{-1} s^3 (1-s^2)^{3/2} \\ &\simeq -43\alpha^2 \dot{m}^{-1} s^3 (1-s^2)^{3/2}, \end{aligned} \quad (16)$$

where $\dot{m} = \dot{M}/\dot{M}_{\text{Edd}}$ is the mass accretion rate in Eddington units, with $\dot{M}_{\text{Edd}} = 1.39 \times 10^{18} m$ g/s, (for a nominal $\eta = 0.1$), $r_{NS} \approx 3$. Note that $-j$ could be very large at low \dot{m} .

We now check under what conditions the approximations we made earlier are valid. First, we neglected the term $v dv/dR$ in equation (2). This is obviously valid since the self-similar solution has $v = \text{constant}$.

Second, we assumed that $|\dot{J}| \gg |\dot{M}\Omega R^2|$ in equation (3). Using (16) this condition may be cast into the form $|j| \gg sr^{1/2}/\sqrt{3}$, or equivalently,

$$\dot{m} \ll 74\alpha^2 s^2 r^{-1/2}. \quad (17)$$

For $\alpha \sim 0.1$, $s \sim 0.3$, and assuming a radial extent of $r \sim 10^2$ for the flow, we require $\dot{m} \lesssim 7 \times 10^{-3}$. A direct numerical simulation (§4) shows that the analytical solution is valid even for values of \dot{m} that are a factor of a few larger than this limit.

Third, we neglected the entropy terms $\rho_{p,e} v T_{p,e} ds_{p,e}/dR$ in equations (4) and (5). For the protons, using the solution (14), we can show that the left-hand-side of equation (4) varies as r^{-4} while the right-hand-side varies $r^{-4.5}$. Thus, with decreasing r , the entropy term becomes progressively less important than the other terms, thereby confirming the validity of the approximation. In the case of the electrons, the entropy is always small since $s_e \sim (m_e T_e / m_p T_p) s_p \ll s_p$.

2.2. Outer Settling Solution

For $r > 10^{2.5}$, both protons and electrons are non-relativistic and the solution described in the previous subsection is not valid. Interestingly, another self-similar solution may be derived for this region of the flow. This solution has a nearly one-temperature plasma with $T_p - T_e \ll T_p, T_e$. The free-free cooling takes the form

$$q^- \sim Q_{\text{ff,NR}} \rho^2 \theta_e^{1/2}, \quad Q_{\text{ff,NR}} = 5\sqrt{2}\pi^{-3/2} \alpha_f \sigma_T \frac{m_e c^3}{m_p^2}, \quad (9')$$

where σ_T is the Thompson cross-section, and the subscript NR stands for non-relativistic. Since the gas is effectively one-temperature, Equation (13) simplifies to

$$q^+ \simeq q^-. \quad (13')$$

We do not need to consider the Coulomb transfer rate q_{Coul} , since this quantity is proportional to $(T_p - T_e)$ and can be adjusted to have the right magnitude with small adjustments of the two temperatures. In the non-relativistic regime, $\theta_e < 1$, $\theta_p \sim (m_e/m_p)\theta_e \ll 1$, and the Coulomb transfer rate is

$$q_{\text{Coul}} = \frac{3}{\sqrt{2}\pi} \frac{m_e}{m_p} \frac{\sigma_T c}{m_p^2} \ln \Lambda \rho^2 \frac{kT_p - kT_e}{\theta_e^{3/2} e^{-1/\theta_e}}. \quad (18)$$

From the condition $q_{\text{Coul}} \simeq q^-$ it follows that

$$kT_p - kT_e \simeq \frac{10}{3\pi^2} \frac{\alpha_f}{\ln \Lambda} \sqrt{m_p m_e} c^2 \theta_e^2 e^{-1/\theta_e}, \quad (19)$$

which is exponentially small for $\theta_e < 1$.

The flow is again described by the self-similar solution (14), with the following two exceptions:

$$\theta_e = \theta_{e0} r^{-1}, \quad \theta_{e0} = \frac{m_p}{m_e} \theta_{p0}, \quad (15b')$$

$$\rho = \rho_0 r^{-2}, \quad \rho_0 = \frac{9\alpha c^2 \Omega_{K0}}{2Q_{\text{ff,NR}}} \frac{\theta_{p0} s^2}{\theta_{e0}^{1/2}} = 0.12 m^{-1} \theta_{p0}^{1/2} \alpha s^2 \text{ g/cm}^3, \quad (15d')$$

where we have used the fact that the total pressure $p = p_p + p_e = 2p_p$.

This solution is valid only if \dot{m} is quite small, cf. equation (17):

$$\dot{m} < 2.2 \times 10^{-3} \alpha_{0.1}^2 s_{0.3}^2 r_3^{-1/2}, \quad (20)$$

where $r_3 = r/10^3$, $\alpha_{0.3} = \alpha/0.3$, and $s_{0.1} = s/0.1$. For greater \dot{m} , a self-similar power-law solution does not exist; numerically computed solutions exhibit non-power-law behavior, as discussed in §4.

3. Properties of the self-similar solution

3.1. Spin-Up/Spin-Down of the Neutron Star

The rate of spin-up of the accreting NS is given by

$$\begin{aligned} \frac{d}{dt} (I_{NS} \Omega) &= \dot{J} - \dot{M} \Omega (R_{NS}) R_{NS}^2 \\ &\simeq -43 s^3 \alpha^2 \dot{M}_{\text{Edd}} \Omega_K (R_{NS}) R_{NS}^2, \end{aligned} \quad (21)$$

where I_{NS} is the moment of inertia of the NS. We have made use of the fact that $|\dot{J}| \gg |\dot{M} \Omega (R_{NS}) R_{NS}^2|$ for the self-similar solution, and used equation (16) for \dot{J} . The negative sign in the final expression implies that the accretion flow spins down the star. The above equation is for an unmagnetized NS. If the NS has a magnetosphere, the inner edge of the accretion flow is at the magnetospheric radius, R_m . In this case, let us define s by $\Omega_{NS} = s \Omega_K (R_m) = s \Omega_K (R_{NS}) (R_m/R_{NS})^{-3/2}$. Substituting this in equation (21) with $I_{NS} = \text{constant}$ and integrating, we obtain

$$s = \frac{s_0}{\sqrt{1 + t/\tau}}, \quad \tau = \frac{I_{NS}}{86 s_0^2 \alpha^2 \dot{M}_{\text{Edd}} R_{NS}^2} \left(\frac{R_m}{R_{NS}} \right)^{-3/2}, \quad (22)$$

where $s_0 = s(t=0)$. The same result is valid for an unmagnetized NS by setting $R_m = R_{NS}$. The quantity τ is the characteristic spin-down time of the NS. For a spherical NS of constant density, $I_{NS} = 2MR_{NS}^2/5 = (0.8 \times 10^{33} \text{ g})mR_{NS}^2$. Substituting this expression, we obtain the spin-down rate $\dot{P}_{NS}/P_{NS} = \tau^{-1}$ with

$$\tau \simeq 6.7 \times 10^{12} s^{-2} \alpha^{-2} \left(\frac{R_m}{R_{NS}} \right)^{-3/2} \text{ s} = 2 \times 10^8 s_{0.1}^{-2} \alpha_{0.1}^{-2} \left(\frac{R_m}{R_{NS}} \right)^{-3/2} \text{ yr}. \quad (23)$$

Note the remarkable fact that the spin-down time scale is independent of the mass of the NS, and the mass accretion rate! For the magnetic case, the rate depends on the radius ratio R_m/R_{NS} .

It is customary to express the spin-down rate as \dot{P}_{NS}/P_{NS}^2 . Writing

$$P_{NS} = \frac{2\pi}{s \Omega_K (R_{NS})} \left(\frac{R_m}{R_{NS}} \right)^{3/2} \quad (24)$$

and $\Omega_K(R_{NS}) \simeq 10^4 m_{1.4}^{-1}$ rad/s, where $R_{NS} = 3R_S$ and $m_{1.4} = M/(1.4M_\odot)$, we obtain

$$\frac{\dot{P}_{NS}}{P_{NS}^2} \simeq 2.4 \times 10^{-10} m_{1.4}^{-1} \alpha^2 s^3 \text{ s}^{-2} = 2.7 \times 10^{-12} m_{1.4}^{-1} \alpha_{0.3}^2 s_{0.5}^3 \text{ s}^{-2}, \quad (25)$$

where $s_{0.5} = s/0.5$. This spin-down rate is in good agreement with observational data on the spin-down of X-ray pulsars for which Yi, Wheeler & Vishniac (1997) invoked ADAFs: 4U 1626-67 has $\dot{P}/P^2 \approx 8 \times 10^{-13} \text{ s}^{-2}$ and $P = 7.7$ s; OAO 1657-415 has $\dot{P}/P^2 \approx 2 \times 10^{-12} \text{ s}^{-2}$ and $P = 38$ s, and GX 1+4 has $\dot{P}/P^2 \approx 3.7 \times 10^{-12} \text{ s}^{-2}$ and $P = 122$ s. Since the spin-down rate is quite sensitive to α and s , the observed data in individual systems can be fitted by small adjustment of these parameters.

3.2. Luminosity

In computing the luminosity of the accretion flow, we must allow for the energy release in both the boundary layer and the self-similar settling zone. We calculate their luminosities separately.

Radiation from the self-similar settling flow may be calculated following the methods described by Popham & Narayan (1995) for a thin disk. This method assumes that the luminosity at a given radius is determined by the local viscous energy production. This is a legitimate approximation for the settling flow in which $q^- = q^+$. Keeping only the dominant terms, we find

$$L_{SS} = \frac{GM_{NS}\dot{M}}{R_{in}} \left(1 + \frac{1}{2}s^2 - js \right) + \dot{M} \int_{P_{in}}^{P_{out}} \frac{dP}{\rho}, \quad (26)$$

where $R_{in} = R_{NS} + \Delta_{BL}$ is the inner radius of the self-similar zone and $\Delta_{BL} \ll R_{NS}$ is the thickness of the boundary layer. Here the first two terms, $(1 + s^2/2)$, represent the luminosity, associated with potential energy of the infalling gas, L_{pot} , the third term $-js$ is the luminosity, associated with the rotational energy extracted from the star, L_{rot} (note, $j < 0$ in the self-similar solution), and the final integral is the ‘‘enthalpy correction’’, L_{enth} . Using the analytical solution (14)–(15) and assuming $P_{\text{out}} = 0$ for simplicity, we obtain

$$L_{\text{pot}} = \dot{M}_{\text{Edd}} c^2 \frac{\dot{m}}{2r_{NS}} \left(1 + \frac{s^2}{2} \right), \quad (27a)$$

$$L_{\text{rot}} = 43 \dot{M}_{\text{Edd}} c^2 \frac{\alpha^2}{2r_{NS}} (1 - \delta)^{1/2} s^4 (1 - s^2), \quad (27b)$$

$$L_{\text{enth}} = -\dot{M}_{\text{Edd}} c^2 \frac{\dot{m}}{2r_{NS}} (1 - s^2). \quad (27c)$$

Note that the leading terms in L_{pot} and L_{enth} cancel each other exactly. The luminosity of the self-similar settling zone is thus

$$L_{SS} \simeq 6.2 \times 10^{34} m r_3^{-1} \dot{m}_{-2} s_{0.1}^2 + 8.9 \times 10^{33} m r_3^{-1} \alpha_{0.1}^2 s_{0.1}^4 \text{ erg s}^{-1}, \quad (28)$$

where $\dot{m}_{-2} = \dot{m}/0.01$, $s_{0.1} = s/0.1$, $r_3 = r_{NS}/3$, and we have assumed $s \ll 1$. Note that luminosity not associated with with dissipation of rotational energy, represented by the first term in equation (28), is much less than the commonly assumed $\sim GM_{NS}\dot{M}/R_{NS}$. This is because the negative enthalpy term has large magnitude, as a result of the fact that the settling flow is akin to a pressure supported, quasi-stationary atmosphere.

The second term in equation (28) is the luminosity of the settling zone. Since the self-similar solution for this zone is independent of \dot{m} , the luminosity too shows no \dot{m} dependence. Indeed, the luminosity remains finite even as $\dot{m} \rightarrow 0$. How is this possible, and where does the energy come from? The answer is that the luminosity of the settling zone is supplied by the central star. As the star spins down, it does work on the accretion flow and the energy released comes out as bremsstrahlung radiation.

The boundary layer luminosity requires a different method of calculation since viscous energy production is negligible in this zone: $\Omega \simeq \text{constant}$, and so $q^+ \propto (d\Omega/dR)^2 \simeq 0$. As the accreting gas cools in the boundary layer, starting from a nearly virial temperature $\sim 10^{12}$ K on the outside down to the NS temperature $\sim 10^7$ K near the surface, the thermal energy in the gas is emitted as radiation. To estimate the luminosity, we use the energy balance equation, which is the sum of equations (4),(5):

$$-q^- = \frac{\rho v}{\gamma - 1} \frac{dc_s^2}{dR} - v c_s^2 \frac{d\rho}{dR} = \frac{\gamma}{\gamma - 1} \rho v \frac{dc_s^2}{dR} - v \frac{dP}{dR}. \quad (29)$$

We can neglect the dP/dR term because the pressure P is essentially constant in the boundary layer. To obtain the luminosity we integrate over the boundary layer

$$L_{BL} = \int q^- 4\pi R^2 dR = - \int \frac{\gamma}{\gamma - 1} 4\pi R^2 \rho v \frac{dc_s^2}{dR} dR = \frac{\gamma}{\gamma - 1} \dot{M} \Delta c_s^2. \quad (30)$$

Since c_s^2 starts from nearly virial value and reaches close to zero, $\Delta c_s^2 \simeq GM_{NS}/R_{NS}$. More precisely, $\Delta c_s^2 = c^2 \Delta(\theta_p + \theta_e) \simeq c^2 \theta_{p0} r_{NS}^{-1}$. Therefore, the boundary layer luminosity is

$$L_{BL} = \frac{\gamma}{\gamma - 1} \dot{M}_{\text{Edd}} c^2 \frac{\dot{m}}{6r_{NS}} (1 - s^2) \approx 1.7 \times 10^{36} m \dot{m}_{-2} r_3^{-1}, \quad (31)$$

where we have assumed $\gamma = 5/3$. The total luminosity of the system is $L = L_{SS} + L_{BL}$.

3.3. Effect of Comptonization

Using the self-similar solution (14),(15), we may readily estimate the electron scattering optical depth and the y -parameter.² The optical depth is

$$\begin{aligned}\tau_{\text{es}} &\simeq \rho\kappa_{\text{es}}R \simeq 10^3\alpha(1-\delta)^{1/2}(1-s^2)^{1/2}s^2r^{-1} \\ &\sim \alpha_{0.1}s_{0.1}^2r^{-1},\end{aligned}\tag{32}$$

where $\kappa_{\text{es}} = \sigma_T/m_p$ is the electron scattering opacity for ionized hydrogen. Since $r \geq 3$, we see that $\tau_{\text{es}} \leq 1/3$ for reasonable parameters and the radiation is optically thin to electron scattering. The y -parameter is

$$\begin{aligned}y &= 16\theta_e^2\tau_{\text{es}} \simeq 2 \times 10^6\alpha(1-\delta)^{-1/2}(1-s^2)^{3/2}s^2r^{-2} \\ &\sim 2 \times 10^3\alpha_{0.1}s_{0.1}^2r^{-2}.\end{aligned}\tag{33}$$

The radius at which $y \sim 1$ is

$$r_c \sim 45\alpha_{0.1}^{1/2}s_{0.1}.\tag{34}$$

Above this radius the inverse Compton scattering is small and the self-similar solution is valid. For $r < r_c$, however, Comptonization is important and the electron temperature profile will be modified from the self-similar form. Since the electron-proton collisions are relatively weak (the plasma is two-temperature), other quantities, e.g., the density, proton temperature, etc., are unaffected. Comptonization is unimportant for low-viscosity flows, $\alpha \lesssim 0.01$ around slowly rotating NSs, $s \lesssim 0.01$, because then $r_c < r_{\text{NS}}$.

3.4. Spectrum

We now estimate the spectrum of radiation emitted from the settling accretion flow. Let us neglect inverse Compton scattering for the moment. The relativistic bremsstrahlung emissivity is approximated as $\epsilon_\nu \propto \rho^2 \exp(-h\nu/kT_e)$ erg cm⁻³ s⁻¹ Hz⁻¹. Therefore the luminosity per unit frequency is

$$\begin{aligned}L_\nu &\propto \int_{R_{\text{NS}}}^{\infty} \rho^2 e^{-h\nu/kT_e} 2\pi R^2 dR \\ &\propto \int_{1/\nu_m}^{\infty} t^{-3} e^{-\nu t} dt \propto \nu^2 \Gamma(-2, \nu/\nu_m),\end{aligned}\tag{35}$$

²Here we just estimate where the effect of Comptonization becomes significant. For better analytical approximations see, for instance, Dermer, Liang, & Canfield (1991); Titarchuk & Lyubarskij (1995). (In the latter paper, the expression for y is not given, but it can be inferred using equation [24]: $y = \tau_{\text{es}}[(\alpha + 3)\theta/(1 + \theta) + 4d_0^{1/\alpha}\theta^2]$.) Comptonization of free-free radiation has also been considered by Titarchuk (1989).

where $\Gamma(a, z) = \int_z^\infty t^{a-1} e^{-t} dt$ is the incomplete gamma-function and $\nu_m = kT_e(R_{NS})/h$ is the maximum frequency. Above ν_m the spectrum falls exponentially and below ν_m it is nearly flat. We may, thus, replace the exponential in the integral with a square function which is equal to unity for $\nu < \nu_m$ and 0 for $\nu > \nu_m$. With this approximation

$$L_\nu \simeq \frac{3}{2} \frac{L_{SS}}{\nu_m} \left(1 - \frac{\nu^2}{\nu_m^2} \right), \quad (36)$$

where $L_{SS} = \int L_\nu d\nu$ is the total luminosity of the self-similar flow, represented by equation (28). The break frequency, ν_m , is roughly given by $h\nu_m \sim 2.7$ MeV for a typical electron temperature $T_{e,\max} \sim 10^{10.5}$ °K [cf., equation (15)]. At a typical x-ray energy, $h\nu \sim 3$ keV, the observed luminosity per decade is

$$\nu L_\nu \simeq 1.7 \times 10^{31} m \alpha_{0.1}^2 s_{0.1}^4 \left(\frac{h\nu}{3 \text{ keV}} \right) \text{ erg s}^{-1}, \quad (37)$$

i.e., $\nu L_\nu \sim 1.5 \times 10^{32}$ for a 300 Hz neutron star ($s_{0.1} \sim 1.6$). The luminosity per decade is much greater at higher photon energies and may be as high as $\sim \text{few} \times 10^{34} - 10^{35}$ erg/s at $h\nu \sim$ MeV.

As shown in the previous section, Comptonization becomes important below the radius r_c . At r_c , $y \approx 1$ and the electron temperature is

$$T_e(r_c) \sim 2.7 \text{ MeV} / \sqrt{r_c} \sim 400 \alpha_{0.1}^{-1/4} s_{0.1}^{-1/2} \text{ keV}. \quad (38)$$

For $r < r_c$, the electron temperature will be determined self-consistently by Compton cooling rather than by bremsstrahlung emission. Computing the spectrum from this region is beyond the scope of the paper. We also do not attempt to calculate the spectrum of the radiation from the boundary layer.

3.5. Bernoulli parameter

It is known that the Bernoulli parameter of the accreting gas in BH ADAFs is positive for a wide range of r (Narayan & Yi 1994, 1995a; Narayan, Kato & Honma 1997), and it has been suggested that the positive Bernoulli parameter may trigger strong winds or jets in these systems (Narayan & Yi 1994, 1995a; Blandford & Begelman 1999, but see Abramowicz et al. 2000). Igumenshchev & Abramowicz (1999, 2000) confirmed with numerical simulations that strong outflows are produced from BH ADAFs when $\alpha \sim 1$.

Normalizing the Bernoulli parameter, Be , by $(\Omega_K R)^2$, and using equations (14),(15), we find that the self-similar settling flow has

$$\begin{aligned} b \equiv \frac{Be}{\Omega_K^2 R^2} &= \frac{1}{v_k^2} \left(\frac{1}{2} v^2 + \frac{1}{2} \Omega^2 R^2 - \Omega_K^2 R^2 + \frac{\gamma}{\gamma - 1} c_s^2 \right) \\ &= \frac{v_0^2}{c^2} r + \frac{s^2}{2} - 1 + \frac{\gamma}{\gamma - 1} \frac{1 - s^2}{3} \end{aligned}$$

$$\simeq -\frac{2\gamma - 3}{3(\gamma - 1)} - \frac{s^2}{2} \frac{3 - \gamma}{3(\gamma - 1)}, \quad (39)$$

where γ is the mean adiabatic index of the flow and in the last expression we have neglected the term in v_0^2 since it is negligible deep inside the settling region.

We see that the second term in the final expression is always negative. This term is proportional to s^2 , which means that a more rapidly spinning NS stabilizes the accretion flow against outflows more effectively than a slower spinning star. The physical explanation is as follows. The centrifugal force increases with increasing s , which has the effect of making it easier for the gas to escape. At the same time, however, the centrifugal force causes the radial infall velocity to decrease, which increases the time available for cooling. The temperature and the gas pressure go down, making the gas more gravitationally bound. The net contribution of the two effects turns out to be negative.

The first term in the last line of equation (39) can be either positive or negative, depending on the value of γ . Combining the two terms, we find that the gas is gravitationally bound and unable to flow out in a wind (i.e. $b < 0$) if the adiabatic index satisfies

$$\gamma > \frac{3(1 - \frac{1}{2}s^2)}{2 - \frac{1}{2}s^2}. \quad (40)$$

For $s^2 \ll 1$, the condition is $\gamma > 1.5$; that is, the the accretion flow can produce a wind and/or a collimated outflow only if $\gamma < 1.5$ and is stable to such outflows if $\gamma > 1.5$. Normally, we expect γ to be close to 5/3 for the accreting gas.

3.6. Stability to Convection

It is well known that if the entropy increases inwards in a gravitationally-bound non-rotating system, the gas is convectively unstable; otherwise the flow is stable. The specific entropy profile in the settling accretion flow around a NS can be readily calculated from equations (4),(5) using (14),(15). This gives

$$\frac{ds}{dR} = \frac{k}{m_p} \frac{1}{\gamma - 1} \frac{d}{dR} \ln \left(\frac{c_s^2}{\rho^{\gamma-1}} \right) = \frac{k}{m_p} \frac{2\gamma - 3}{\gamma - 1} \frac{1}{R}. \quad (41)$$

We see that the entropy increases outwards for $\gamma > 1.5$ and inwards for $\gamma < 1.5$. Hence if $\gamma > 1.5$ the flow is stable against convection, while if $\gamma < 1.5$ the flow is convectively unstable.

In the presence of rotation, the analysis is a little more complicated. Narayan et al. (2000) and Quataert & Gruzinov (2000) discuss the generalization of the Schwarzschild criterion for accretion flows with rotation. If the gas motions are restricted to the equatorial plane of a height-integrated flow, convective stability requires the following effective frequency to be positive:

$$N_{\text{eff}}^2 = N^2 + \kappa^2 > 0, \quad (42)$$

where N is the Brunt-Väisälä frequency and κ is the epicyclic frequency, $\kappa = \Omega$ for $\Omega \propto R^{-3/2}$. For a power-law flow with $\rho \propto R^{-a}$ and $\Omega(R) = s\Omega_K \propto R^{-3/2}$ with $s^2 = 1 - (1+a)c_0^2$, this criterion may be written as follows (see Narayan et al. 2000 for more discussion)

$$N_{\text{eff}}^2 = \Omega_K^2 \left(-[(\gamma + 1) - a(\gamma - 1)] \frac{(1+a)c_0^2}{\gamma} + 1 \right) > 0. \quad (43)$$

Since for the self-similar settling solution $a = 2$, the stability criterion (43) becomes

$$N_{\text{eff}}^2 = \frac{\Omega_K^2}{\gamma} [(2\gamma - 3) + s^2(3 - \gamma)] > 0 \quad (44)$$

which yields that the flow is convectively stable if

$$\gamma > \frac{3(1 - s^2)}{2 - s^2}. \quad (45)$$

This condition is different from the stability criterion against outflows, given in equation (40).

Following the techniques developed by Quataert & Gruzinov (2000), Narayan et al. (2000) have also presented a more general analysis of convection in a self-similar accretion flow. This analysis, which does not restrict motions to lie in the equatorial plane, assumes that v_ϕ and c_s are independent of the polar angle θ (as is valid for a marginally convectively stable system, cf Quataert & Gruzinov 2000). Narayan et al. (2000) find that the most unstable region of the flow is near the rotation axis, $\theta = 0, \pi$. They show that the marginal stability criterion for this polar fluid coincides with the condition for the positivity of the Bernoulli parameter. That is, a flow which is convectively stable at all θ has a negative Bernoulli parameter, while a flow which is convectively unstable for at least some values of θ has a positive Bernoulli parameter. (The Bernoulli parameter itself is independent of θ .)

We have verified this result for the solutions presented in this paper. Specifically, when we apply to our solution the more general convective stability criterion given by equation (A9) of Narayan et al. (2000), we recover the condition (40) above, namely that the self-similar flow is convectively stable if and only if

$$\gamma > \frac{3(1 - \frac{1}{2}s^2)}{2 - \frac{1}{2}s^2}. \quad (46)$$

4. Comparison with Numerical Results

We have numerically solved the system of height-integrated two-temperature fluid equations (1)–(5) with boundary conditions. In the energy equations we assume that viscous dissipation only heats the protons (i.e. $\delta = 0$). We include energy transfer from protons to electrons via Coulomb collisions, and we take the cooling of electrons to be purely by free-free emission, as discussed in §2. For these processes we use the expressions given in Narayan & Yi (1995b), which smoothly

interpolate between the regimes of non-relativistic and relativistic electrons. We take into account the variation of the electron adiabatic index γ_e with temperature (Chandrasekhar 1939; Esin et al. 1997), using a simple interpolation formula from Gammie & Popham (1998). We assume that the protons have $\gamma_p = 5/3$.

We employ the gravitational potential of Paczyński & Wiita (1980) to mimic the effect of strong gravity near the NS surface. In this potential the Keplerian angular velocity takes the form

$$\Omega_K^2 = \frac{GM}{(R - R_S)^2 R}. \quad (47)$$

Note that the analytical work presented in the previous sections is based on a Newtonian potential.

We specify the boundary conditions as follows. We take the outer boundary of the flow to be at $r_{\text{out}} = 10^6$. At this radius we specify that the angular velocity is equal to its value in the self-similar ADAF solution of Narayan & Yi (1994), and that the proton and electron temperatures are both equal to the self-similar ADAF temperature. We assume that the accreting star is a $1M_\odot$ neutron star with a radius $R_{NS} = 3R_S = 8.85$ km, unless stated otherwise. At $R = R_{NS}$, we specify the value of the NS spin parameter, $s = \Omega_{NS}/\Omega_K(R_{NS})$, and we require the proton temperature of the flow to be $T = \text{few} \times 10^7$ K $\ll T_{\text{virial}}$. (We do not assume that the electron and proton temperatures are equal, but in fact they are equal.) We do not constrain the density of the gas in any way at either boundary.

The numerical problem as posed here has a family of solutions characterized by three dimensionless parameters: the mass accretion rate \dot{m} (in Eddington units), the NS spin s (in units of the Keplerian angular velocity at the NS surface), and the viscosity parameter α . The angular momentum flux \dot{J} , or equivalently the dimensionless flux $j = \dot{J}/\dot{M}\Omega_K(R_{NS})R_{NS}^2$, is an eigenvalue of the problem.

Figure 1 shows representative solutions for $\alpha = 0.1$ and a range of values of \dot{m} and s . The solutions clearly have three radial zones. For $r > 10^{2.5}$, there is a one-temperature zone in which the gas properties vary roughly as power-laws of the radius. For $r < 10^{2.5}$, there is a second power-law zone with a two-temperature structure. Finally, close to the NS, the flow has a boundary layer region. In this final region, the gas experiences run-away cooling, the velocity falls precipitously, and the density increases very rapidly. This region of the flow does not have power-law behavior.

The numerical solutions are unreliable in the boundary layer; thermal conduction (not included in the calculations) is probably very important here, and optical depth effects (also not included) will modify the radiation properties significantly. The solutions are suspect also in the inner region of the two-temperature power-law zone, where Comptonization is likely to be important. Outside these regions, however, the numerical solution is expected to be accurate.

The numerical results in the two-temperature power-law zone below $r \sim 10^{2.5}$ agree quite well with the analytical solution presented in §2.1. Curves corresponding to a given value of s and different values of \dot{m} coincide with one other to very good accuracy, as predicted by the analytical

solution. This is best seen in the profiles of ρ and Ω . Changing s causes an up/down shift of the curves but does not affect the slopes of the curves. The temperature profiles are sensitive to the spin s , especially for large values of s . The radial velocity varies approximately as $v \propto \dot{m}$ and is roughly consistent with $v \propto r^0$ for $s > 0.1$.

For $r > 10^{2.5}$, the numerical solutions are in reasonable agreement with the one-temperature self-similar solution described in §2.2. The agreement is less perfect than in the previous zone. This is primarily because the analytical solution requires a very low value of \dot{m} in order to be valid as far out as the outer radius $r \sim 10^6$ [cf., equation (20)]. The numerical models shown have larger values of \dot{m} than this limit.

As we discussed in §2 and §3, the transport of angular momentum in a hot settling flow differs dramatically from the well-known behavior of a thin disk. The solid line in Figure 2 indicates the dependence of the dimensionless angular momentum eigenvalue j as a function of the dimensionless NS spin s . The long-dashed line indicates the corresponding results for a thin disk (Popham & Narayan 1991), where $j \simeq +1$ for most values of s , and goes negative only for stars nearly at break-up. In contrast, in the settling flow, j is negative for almost all values of s . For the particular choice of parameters, namely $\alpha = 0.1$, $\dot{m} = 0.01$, $s \sim \text{few} \times 10^{-1}$, we find that $j \sim -\text{few}$.

The short-dashed line in Figure 2 shows the analytical formula for j , as given in equation (16). The agreement with the numerical results is good for a wide range of s below about 0.5. For $s > 0.5$, the numerically determined j levels off at a constant negative value, whereas the analytical result shows $|j|$ decreasing rapidly. The main reason for the discrepancy is the neglect of the ram pressure term in the radial momentum equation in the analytical work. Note the interesting fact that super-Keplerian accretion ($s > 1$) is, in principle, possible (provided one can arrange to have a star with super-Keplerian rotation). In a super-Keplerian flow, the ram pressure of the infalling gas supplies the radial momentum needed to push the gas onto the NS. For extremely small $s \ll 0.1$, the numerical solutions show j to be slightly positive; we find $j \sim 10^{-3}$, as indicated in the lower panel in Figure 2. Here again the self-similar solution, which predicts a small negative value for j , breaks down. For very small s , the \dot{J} term in equation (3) is comparable to or smaller than the $\dot{M}\Omega R^2$ term which was omitted in deriving the analytical solution. This is the reason for the discrepancy. The precise value of s at which the analytical solution breaks down depends on the choice of parameters (α , \dot{m}), but is essentially independent of the outer radius. Thus, the transport of angular momentum through the flow and the spin-down of the star are determined by the boundary conditions at the stellar surface, and not by the outer boundary of the flow.

One of the most surprising features of the self-similar solution is that the angular momentum flux \dot{J} is independent of \dot{m} ; equivalently, the dimensionless eigenvalue j is $\propto \dot{m}^{-1}$. The solid line in Figure 3 is a plot of $-j$ as a function of \dot{m} for a flow with $\alpha = 0.1$ and $s = 0.3$, as determined from the numerical solutions. The dashed line indicates for comparison the analytical scaling, $j \propto \dot{m}^{-1}$, with the proportionality constant given in equation (16). Note the very good agreement between the numerical results and the analytical self-similar solution.

The highest value of \dot{m} up to which we could obtain a numerical solution is $\dot{m}_{\text{crit}} = 0.0313$. Beyond this critical value, there is no hot solution. (The value of \dot{m}_{crit} depends on s , α and r_{out} .) For larger \dot{m} , the density in the flow is so high that there is runaway free-free cooling and the gas is unable to remain hot. We presume that the accretion then occurs via a thin accretion disk.

Figure 4 plots, for selected values of \dot{m} , the luminosity per logarithmic interval of D , where D is the fractional distance from the NS surface:

$$D = \frac{(R - R_{NS})}{R_{NS}}. \quad (48)$$

We see that the luminosity at the peak of the curve is very insensitive to \dot{m} . The emission in the peak corresponds to radiation from the settling flow. This emission represents energy released by the spin-down of the NS, and its luminosity is independent of \dot{m} [cf. equation (28)]. For radii below the peak, the curves do show a dependence on \dot{m} . The radiation here corresponds to boundary layer emission, which is proportional to \dot{m} according to equation (31).

All the models described above have $R_{NS} = 3R_S$. However, different equations of state predict slightly different NS radii, $R_{NS} = 2 - 4R_S$. We have computed numerical models for this range of R_{NS} and we find that the subsonic settling solution exists for the whole range. Qualitatively, the solutions with different R_{NS} are very similar. As R_{NS} decreases, the peak temperature is higher, as expected for the deeper potential.

5. Relationship of the Settling Flow to an ADAF

The accretion solution we have discussed so far radiates all the energy dissipated by viscosity, and is therefore “cooling-dominated.” On the other hand, it is known that a hot flow around a black hole is an “advection-dominated” accretion flow (ADAF). Both solutions have a two-temperature structure for $r \lesssim 10^{2.5}$ and both are very hot (nearly virial) for all r . How are these two types of accretion flows related to each other?

By solving the equations numerically for different boundary conditions, we have found that the two solutions are part of a single sequence of solutions in which the spin of the star, s , plays a pivotal role as a control parameter. For relatively rapidly rotating stars, with $s \gtrsim 0.1$, we obtain the settling solution in our numerical experiments. However, as s is decreased, we find that the settling solution smoothly transforms to an ADAF-type solution, which becomes well-established for $s \lesssim 0.01$. The transition is not sharp, so it is difficult to identify a specific transition point $s = s_t$ at which the transformation occurs. Numerical experiments indicate that the value of s_t (however it is defined) is not very sensitive to R_{out} , γ , and \dot{m} and is, roughly, $s_t \sim 0.04 - 0.06$.

The change of the nature of the flow as s is varied is illustrated in Fig. 5. The solid and dotted curves correspond to two solutions with $s = 0.3$ and $s = 0.01$, respectively, with all other boundary conditions being the same. We see that the solutions are markedly different from each other. This

is most clearly seen in the profiles of density, where the $s = 0.3$ model has a logarithmic slope of -2, as appropriate for the cooling-dominated settling solution described in this paper, and the $s = 0.01$ model has a slope of -3/2, as expected for a standard self-similar ADAF (Narayan & Yi 1994, 1995a). There is a similar difference also in the profiles of the radial velocity, where the two solutions have logarithmic slopes of -1/2 and 0, respectively.

An interesting feature of the $s = 0.01$ ADAF-type solution is that it consists of two distinct segments. For large radii (in Fig. 5, for radii outside $r \sim 20$), the flow corresponds to the standard ADAF discussed in the literature, with the scalings

$$\rho \propto r^{-3/2}, \quad c_s^2 \propto r^{-1}, \quad \Omega \propto r^{-3/2}, \quad v \propto r^{-1/2}. \quad (49)$$

However, at smaller radii, the numerical solution indicates the presence of a second advection-dominated zone, a “settling ADAF,” which was first seen in numerical calculations described in Narayan & Yi (1994). This settling ADAF is seen in Fig. 5 as a zone that lies between the boundary layer region and the outer standard ADAF, with different slopes for ρ and v . The radial extent of the settling ADAF zone may be quite large and, in general, depends on the flow parameters and boundary conditions.

A self-similar model of the settling ADAF may be readily obtained as follows. In an ADAF, energy is not radiated, therefore $q^- = 0$. Close to the star $\Omega \simeq \text{constant}$, therefore $q^+ = 0$. Equations (4), (5) then simplify to the condition of entropy conservation, $ds/dR = 0$, which yields $c_s^2 \propto \rho^{\gamma-1}$. As the material settles on the star, its radial velocity decreases and we have $v \ll v_{ff}$, $\Omega \ll \Omega_K$. Then, from equation (2), it follows that the temperature of the gas is nearly virial. Other quantities are determined straightforwardly, so that we have

$$\rho \propto r^{\frac{1}{\gamma-1}}, \quad c_s^2 \propto r^{-1}, \quad \Omega \sim \text{const.}, \quad v \propto r^{-\frac{2\gamma-3}{\gamma-1}}. \quad (50)$$

The infall velocity decreases with radius if $\gamma < 1.5$, and increases if $\gamma > 1.5$. To highlight the difference between the standard ADAF and the settling ADAF, we have chosen $\gamma = 4/3$ in the solutions shown in Fig. 5.

Finally, the long-dashed curves in Fig. 5 correspond to a solution with $s = 0.3$ for which we have increased the outer boundary value of T by a factor of 10. We see that the solution in the interior is not sensitive to the outer boundary conditions (within a reasonable range, of course).

6. Summary and Discussion

In this paper, we have presented analytical and numerical solutions that describe a hot, viscous, two-temperature accretion flow onto a neutron star (NS). The results are relevant also for accretion onto other compact stars with a surface, e.g. white dwarfs. To our knowledge, this is the first study of viscous fluid dynamics for a hot flow around a NS.

The presence of a surface modifies the nature of the flow relative to the case of a black hole. We show that the accretion flow has an extended settling region in which the radial velocity v is constant; v is also small relative to the local free-fall velocity. The density in the settling region varies as $\rho \propto r^{-2}$, and the angular velocity has a Keplerian scaling, $\Omega = s\Omega_K \propto r^{-3/2}$, with s being a constant. Here, r is the radius in Schwarzschild units, and the value of s is set by the spin of the NS: $s = \Omega_{NS}/\Omega_K(r_{NS})$. At the inner edge of the settling region, there is a narrow boundary layer in which the velocity falls extremely rapidly and the density increases sharply to match the surface density of the NS.

The settling region consists of two distinct zones. In the inner zone, $r \lesssim 10^{2.5}$, the gas is two-temperature, with the proton temperature varying as $T_p \propto r^{-1}$ and the electron temperature varying as $T_e \propto r^{-1/2}$. These scalings are derived assuming that electrons radiate primarily by free-free emission and that energy transfer from protons to electrons occurs via Coulomb collisions. We have derived a completely general analytical self-similar solution for this region which agrees well with numerical results.

In the outer zone of the settling region, $r \gtrsim 10^{2.5}$, the gas is one-temperature, $T_p \approx T_e \propto r^{-1}$; here again, we derive an analytical self-similar solution which agrees reasonably well with numerical results.

The most surprising feature of the settling region is that nearly all the gas properties are independent of the mass accretion rate \dot{m} ; only the radial velocity shows a dependence: $v \propto \dot{m}$. Since the density and temperature are independent of \dot{m} , the luminosity is also independent of \dot{m} . Indeed, the settling solution is valid—with a finite luminosity—even in the limit when $\dot{m} \rightarrow 0$. Clearly, the luminosity does not originate from the gravitational release of energy as mass accretes onto the NS.

The magnitude of the luminosity is very sensitive to the spin parameter s of the NS, varying as the fourth power of this quantity, equation (28). For $s \sim 0.1$, as appropriate for the millisecond X-ray pulsar, SAX J1808.4-3658, the model predicts an X-ray (few keV) luminosity $\nu L_\nu \sim 10^{32}$ erg s⁻¹ (§3.2). This estimate does not include the contribution from Comptonization in the inner regions of the flow, which might increase the X-ray luminosity by an undetermined amount. We note that quiescent X-ray luminosities of soft X-ray transients, including SAX J1808.4-3658, are generally in the range $\nu L_\nu \lesssim 10^{33}$ erg s⁻¹ (Narayan, Garcia & McClintock 1997; Asai et al. 1999; Menou et al. 1999; Stella et al. 2000).

The angular momentum flux \dot{J} in the settling solution is dominated by the viscous transport term rather than the advection term $\dot{M}\Omega_K R^2$. Consequently, \dot{J} is negative, i.e. the angular momentum flux is oriented outward, and the accretion flow spins down the star. The analytical solution predicts that spin-down occurs for all values of the spin parameter s of the central star. The numerical solutions by and large confirm this; for plausible parameters, spin-up is seen only for extremely small values of the spin parameter, $s < 0.005$ (cf Fig. 2). (The exact value of s at which \dot{J} changes sign depends on α and \dot{m} , but is relatively independent of the position of the outer

edge of the flow.) This behavior is very different from the case of a thin accretion disk (Popham & Narayan 1991; Paczyński 1991), where one finds that the star is spun-up for nearly all values of s , and spin-down occurs only for s close to unity (break-up limit).

Another surprising feature of the settling solution is that \dot{J} , like nearly all other quantities, is independent of \dot{m} . Indeed, the settling zone behaves like a stationary zone (since v is very small), and essentially acts like a conventional “brake,” slowing down the star by viscosity. The brake can operate even if $\dot{m} \rightarrow 0$, so long as there is a static atmosphere of the self-similar form and there is a sink for the angular momentum, say an external medium, at large r . Furthermore, the luminosity of the settling flow is almost entirely from the energy released by the viscous braking action. That is, the luminosity ultimately is fed by the loss of rotational kinetic energy of the star, and not by gravity.

This result has an interesting consequence. In accretion flows around black holes, one defines an efficiency factor η by comparing the accretion luminosity L_{acc} to the rest mass energy of the accreting gas, $\eta \equiv L_{acc}/\dot{M}c^2$. It is well-known that $\eta = 0.06$ for a thin accretion disk around a Schwarzschild black hole and that the value increases to $\eta = 0.42$ for a maximally rotating Kerr hole. A number of interesting ideas have been discussed in the literature for increasing the efficiency of an accretion flow around a black hole; these involve tapping the rotational energy of the black hole using magnetic fields or viscosity (Blandford & Znajek 1977; Krolik 1999; Gammie 1999). The general relativistic dragging of inertial frames by the spinning hole plays an important role in the mechanism of (Blandford & Znajek 1977).

For the hot settling solution described in this paper, the luminosity is almost entirely from the rotational energy of the star. Since L_{acc} is independent of \dot{m} , the efficiency scales as $\eta \propto \dot{m}^{-1}$ and $\eta \rightarrow \infty$ as $\dot{m} \rightarrow 0$. Thus, it would appear that accretion flows can tap the rotation energy of a star with a surface more easily than the energy of a spinning black hole. Sibgatullin & Sunyaev (2000) showed that the extraction of rotational energy of a NS may result in very high boundary layer efficiencies, up to $\eta \sim 0.67$, in the counter-rotating NS–thin disk systems, as well. As in the case of the black hole, the energy extraction works best when the star is spinning rapidly: $\eta \propto s^4$. Interestingly, the energy extraction is not a general relativistic effect — our analytical solution is based entirely on Newtonian physics.

Yi, Wheeler & Vishniac (1997) and Yi & Wheeler (1998) recently suggested that the sudden torque-reversal events seen in some accretion-powered pulsars may be due to the accretion flow switching between a Keplerian thin disk and a hot a sub-Keplerian state akin to an ADAF. Our work lends support to this suggestion. We find that the torque does reverse in sign between a thin accretion disk and a hot settling flow for almost any reasonable stellar spin parameter. We also find that the magnitude of the spin-down torque exerted by the settling flow is comparable to the measured value of the torque in torque-reversing pulsars (§3.1).

It is worth emphasizing that the settling solution described here is quite distinct from the self-similar ADAF solutions derived for black hole accretion (Narayan & Yi 1994, 1995a; Honma

1996; Kato & Nakamura 1998; Blandford & Begelman 1999; Manmoto et al. 2000). All the black hole solutions described in the literature have density varying relatively mildly with radius: $\rho \propto r^{-3/2} - r^{-1/2}$. Our settling solution has $\rho \propto r^{-2}$. Also, the black hole solutions are advection-dominated, whereas our solution radiates essentially all the energy it generates through viscous dissipation. There are also, as we now discuss, significant differences in the sign of the Bernoulli parameter and in the stability to convection.

Narayan & Yi (1994, 1995a) showed that their self-similar ADAF solution has a positive Bernoulli parameter so long as the adiabatic index γ of the gas is less than $5/3$. They argued on the basis of this that ADAFs are likely to have strong outflows and winds (but see Abramowicz et al. 2000). Such strong outflows were confirmed with numerical simulations by Igumenshchev & Abramowicz (1999, 2000); they found outflows for large values of the viscosity parameter: $\alpha \sim 1$. Blandford & Begelman (1999) developed a self-similar model with inflow and outflow (the ADIOS model). For the settling solution described in this paper, the Bernoulli parameter is positive only if γ is less than γ_{crit} , where $\gamma_{crit} = 1.5$ for a slowly-spinning star and is smaller than 1.5 for a rapidly-spinning star [cf equation (40)]. Since the hot ionized two-temperature gas in the flow is likely to have γ close to $5/3$ at most radii, we expect the Bernoulli parameter to be generally negative. Therefore, we do not expect a strong outflow. Of course, this conclusion assumes that we do not have dynamically important magnetic fields in the flow.

Narayan & Yi (1994, 1995a) also showed that their ADAFs are convectively unstable for a wide range of conditions. The convective instability has been seen in numerical simulations in which the viscosity parameter is assigned a low value: $\alpha \lesssim 0.1$ (Igumenshchev, Chen, & Abramowicz 1996; Igumenshchev & Abramowicz 1999, 2000; Stone, Pringle, & Begelman 1999; Igumenshchev, Abramowicz, & Narayan 2000). Self-similar solutions for convection-dominated accretion flows (CDAFs) have been derived by Narayan et al. (2000) and Quataert & Gruzinov (2000). For the settling solution described in this paper, we find that the gas is convectively unstable only for the same low values of γ for which the Bernoulli parameter is positive. (Narayan et al. 2000 showed that, in general, for self-similar flows the criterion for the Bernoulli parameter to be positive is the same as the criterion for the flow to be convectively unstable, cf. §3.6.) Thus, we do not expect hot settling flows around NSs to be convectively unstable, or to have a distinct CDAF mode of settling.

From numerical experiments we have discovered the interesting property that the settling flow can continue well inside the last stable orbit (down to at least $r_{NS} \sim 2$) and yet remain subsonic at all radii. This is despite the fact that the numerical models employ a pseudo-Newtonian potential which mimic the last stable orbit for test particles. We find that the structure of the flow is qualitatively similar for flows with $r_{NS} < 3$ and $r_{NS} > 3$. This is very different from black hole ADAFs which become supersonic close to the central object.

We have also shown (§5) that the settling solution and the ADAF are not two physically distinct solutions, but are related to each other. As the neutron star spin is decreased, we find that

the settling flow smoothly transforms to an ADAF-type solution. The transformation proceeds over the spin range $s \sim 0.01 - 0.1$.

The settling solution is hot but cooling-dominated. It is thus most closely related to the two-temperature solution discovered by Shapiro, Lightman & Eardley (1976). The SLE solution is known to be thermally unstable (Piran 1978; Wandel & Liang 1997; Narayan & Yi 1995b), so one may wonder about the thermal stability of our settling solution. We defer discussion of this important topic to a future paper.

Could there be non-settling solutions around NSs, and could such flows be more analogous to the black hole ADAF, ADIOS, and CDAF solutions? Indeed this is possible if the NS radius is small enough. We could imagine, for instance, a standard black hole-like flow around a NS, which makes a sonic transition to a supersonic state, and then stops suddenly at a standing shock at the surface of the NS. Such a solution would be dynamically consistent, and, except for the shock, would be very similar to a black hole flow. However, for such a solution to exist, one requires the radius of the NS to be smaller than the sonic radius of the flow. The latter radius is estimated to be in the range $r_{sonic} \sim 2 - 5$, depending on the value of α (Narayan, Kato & Honma 1997; Popham & Gammie 1998), whereas NS radii are in the range $r_{NS} \sim 2 - 4$ for typical NS equations of state. Thus, for some choices of α and some equations of state, r_{NS} could be smaller than r_{sonic} . In such cases, we could have four different hot solutions around a NS: (i) we could have the self-similar settling solution of the kind presented in this paper (as we discussed in §4, we find subsonic settling solutions for any choice of R_{NS} in the range $2 - 4R_S$); or (ii) we could have a Narayan, Kato & Honma (1997)–like ADAF solution with a shock at the NS surface; or (iii) we could have a Blandford & Begelman (1999)–like ADIOS solution with a shock at the NS surface; or (iv) we could have a Narayan et al. (2000) and Quataert & Gruzinov (2000)–like CDAF, again with a shock at the NS surface. In the latter three cases, we expect the NS to be *spun-up* rather than spun-down by the accretion flow, and we also expect the radiative efficiency to be close to the standard value for a NS, namely $\eta \sim 0.1 - 0.5$. The spectrum of the radiation is also likely to be very different in the four models. This may provide a way to distinguish which if any of these possibilities is found in nature.

In addition to the above possibilities, yet other flow configurations may be possible when we allow for the multi-dimensional nature of the flow. These could be explored with numerical hydrodynamics simulations.

This work was supported in part by grants PHY 9507695 and AST 9820686 from the National Science Foundation.

REFERENCES

Abramowicz, M. A., Czerny, B., Lasota, J. P., & Szuszkiewicz, E. 1988, ApJ, 332, 646

- Abramowicz, M. A., Chen, X., Kato, S., Lasota, J.-P., & Regev, O. 1995, *ApJ*, 438, L37
- Abramowicz, M. A., Lasota, J.-P., & Igumenshchev, I. V. 2000, *MNRAS*, 314, 775
- Asai, T., Takahashi, K., & Dotani, T. 1999, *AN*, 320, 347
- Blandford, R. D., & Begelman, M. C. 1999, *MNRAS*, 303, L1
- Blandford, R. D., & Znajek, R. L. 1977, *MNRAS*, 179, 433
- Chandrasekhar, S. 1939, *Introduction to the Study of Stellar Structure* (New York: Dover)
- Chen, X., Abramowicz, M. A., Lasota, J.-P., Narayan, R., & Yi, I. 1995, *ApJ*, 443, L61
- Dermer, C. D., Liang, E. P., & Canfield, E. 1991, *ApJ*369, 410
- Esin, A. A., McClintock, J. E., & Narayan, R. 1997, *ApJ*, 489, 865
- Gammie, C. F., & Popham, R. 1998, *ApJ*, 498, 313
- Gammie, C. F. 1999, *ApJ*, 522, L57
- Honma, F. 1996, *PASJ*, 48, 77
- Ichimaru, S. 1977, *ApJ*, 214, 840
- Igumenshchev, I. V., Chen, X., & Abramowicz, M. A. 1996, *MNRAS*, 278, 236
- Igumenshchev, I. V., & Abramowicz, M. A. 1999, *MNRAS*, 303, 309
- Igumenshchev, I. V., & Abramowicz, M. A. 2000, *astro-ph/0003397*
- Igumenshchev, I. V., Abramowicz, M. A., & Narayan, R. 2000, *astro-ph/0004006*
- Kato, S., Fukue, J., & Mineshige, S. 1998, *Black-Hole Accretion Discs* (Kyoto: Kyoto University Press)
- Kato, S., & Nakamura, K. E. 1998, *PASJ*, 50, 559
- Krolik, J. H. 1999, *ApJ*, 515, L73
- Manmoto, T., Kato, S., Nakamura., & Narayan, R. 2000, *ApJ*, 529, 127
- Menou, K., Esin, A. A., Narayan, R., Garcia, M. R., Lasota, J.-P., & McClintock, J. E. 1999, *ApJ*, 520, 276
- Narayan, R., Garcia, M. R., & McClintock, J. E. 1997, *ApJ*, 478, L79
- Narayan, R., Igumenshchev, I. V., & Abramowicz, M. A. 2000, *astro-ph/9912449*

- Narayan, R., Kato, S., & Honma, F. 1997, *ApJ*, 476, 49
- Narayan, R., Mahadevan, R., & Quataert, E. 1998, in *Theory of Black Hole Accretion Discs*, eds. M.A. Abramowicz, G. Bjornsson, & J. E. Pringle (Cambridge University Press), p. 148
- Narayan, R., & Yi, I. 1994, *ApJ*, 428, L13
- Narayan, R., & Yi, I. 1995, *ApJ*, 444, 231
- Narayan, R., & Yi, I. 1995, *ApJ*, 452, 710
- Paczyński, B. 1991, *ApJ*, 370, 597
- Paczyński, B., & Wiita, P. J. 1980, *A&A*, 88, 23
- Popham, R., & Gammie, C. F. 1998, *ApJ*, 504, 419
- Popham, R., & Narayan, R. 1991, *ApJ*, 370, 604
- Popham, R., & Narayan, R. 1995, *ApJ*, 442, 337
- Quataert, E., & Gruzinov, A. 2000, *astro-ph/9912440*
- Sibgatullin, R. N., & Sunyaev, R. A. 2000, *Astronomy Lett.*, 26, 699
- Stella, L., Campana, S., Mereghetti, s., Ricci, D., & Israel, G. L. 2000, *ApJ*, in press (*astro-ph/0005429*)
- Stone, J. M., Pringle, J. E., & Begelman, M. C. 1999, 310, 1002
- Titarchuk, L. 1989, *Astrophysics* (tr. *Astrofizika*), 29, 634
- Titarchuk, L., Lapidus, I., & Muslimov, A. 1998, *ApJ*, 499, 315
- Titarchuk, L. & Lyubarskij, Yu. 1995, *ApJ*, 450, 876
- Titarchuk, L. & Osherovich, V. 1999, *ApJ*, 518, L95
- Yi, I., Narayan, R., Barret, D., & McClintock, J. E. 1996, *A&AS*, 120, 187
- Yi, I., Wheeler, J. C., & Vishniac, E. 1997, *ApJ*, 481, L51
- Yi, I., & Wheeler, J. C. 1998, *ApJ*, 498, 802
- Yuan, F. 1999 *ApJ*, 521, L55

Fig. 1.— Profiles of density ρ (g cm^{-3}), proton temperature T_p ($^{\circ}\text{K}$), electron temperature T_e ($^{\circ}\text{K}$), angular velocity Ω (in units of the Keplerian angular velocity at the NS radius R_{NS}), and radial velocity v (in units of c) for accretion flows with $\alpha = 0.1$ and $(\dot{m}, s) = (0.01, 0.3)$ – solid line, $(0.0001, 0.3)$ – short-dashed line, $(0.01, 0.1)$ – medium-dashed line, $(0.01, 0.7)$ – long-dashed line.

Fig. 2.— The solid curve corresponds to the dimensionless specific angular momentum flux j , shown as a function of the dimensionless spin of the NS s , for $\dot{m} = 0.01$ and $\alpha = 0.1$. The long-dashed line is $j(s)$ for the thin disk case, taken from Popham & Narayan (1991). The short-dashed curve corresponds to the analytical self-similar solution, equation (16). The lower panel gives a close-up of the small- s region of the upper plot.

Fig. 3.— Variation of the angular momentum flux parameter $-j$ as a function of \dot{m} for $s = 0.3$, $\alpha = 0.1$. The solid curve corresponds to the results from numerical computations, and the dashed curve corresponds to the analytical self-similar solution.

Fig. 4.— Luminosity (erg/s) of the settling flow per unit logarithmic interval of $D = (R - R_{NS})/R_{NS}$ for $\alpha = 0.1$, $s = 0.3$. The curves correspond to different choices of the mass accretion rate: from below, $\dot{m} = 0.0001, 0.001, 0.003, 0.01, 0.02$. A substantial part of the luminosity is independent of \dot{m} ; this part is from the settling flow. There is some weak dependence of the luminosity on \dot{m} at small D , due to boundary layer emission, and at large D , due to non-self-similar behavior of the numerical solution.

Fig. 5.— Same as in Fig. 1 for $\gamma = 4/3$ and $s = 0.3$ (solid curve) and $s = 0.01$ (dotted curve). Corresponding self-similar slopes for an ADAF and the settling flow are also show. The long-dashed curves represent the same solution as the solid curve, but with ten times higher temperature at R_{out} .

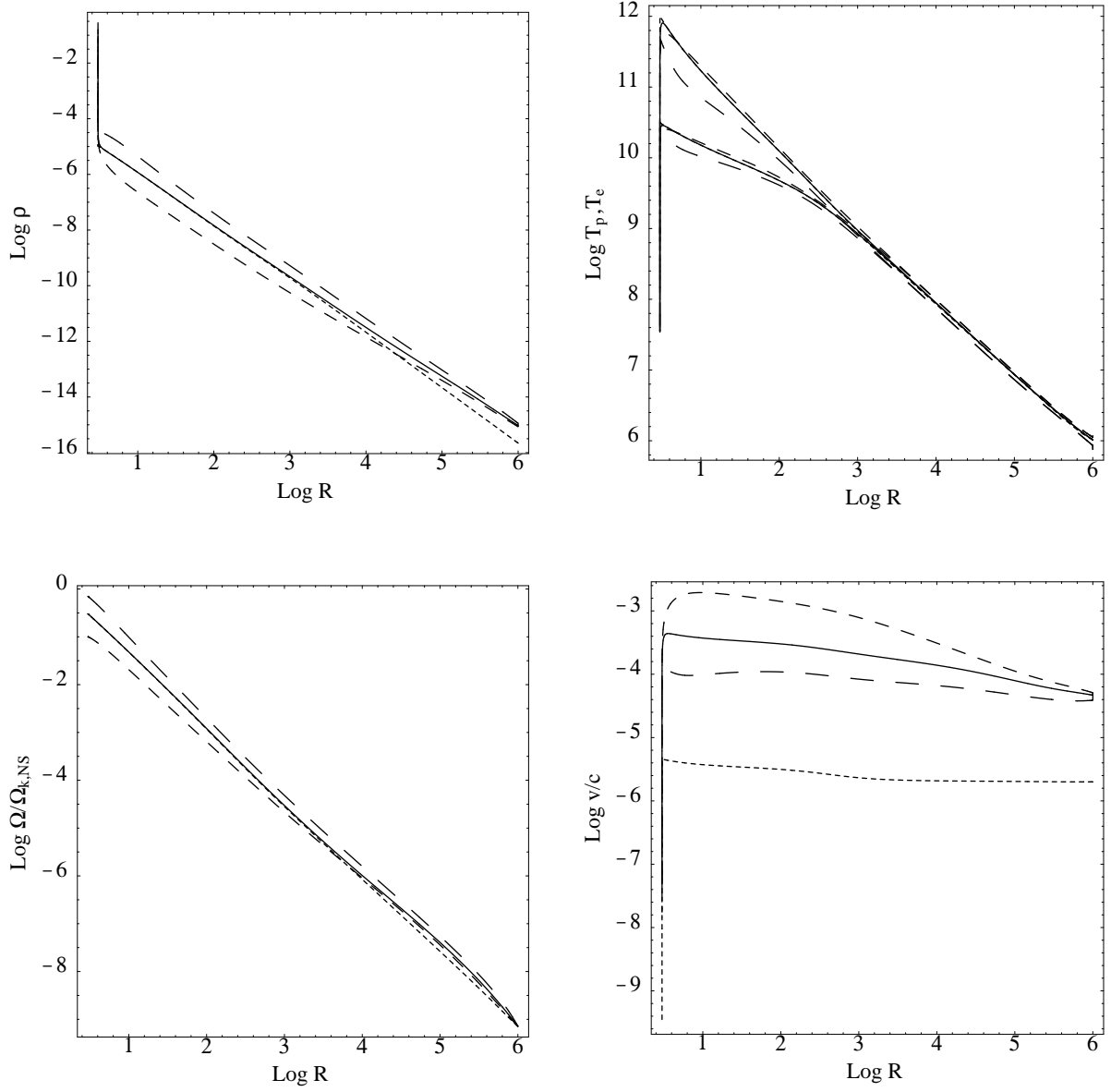


Fig. 1

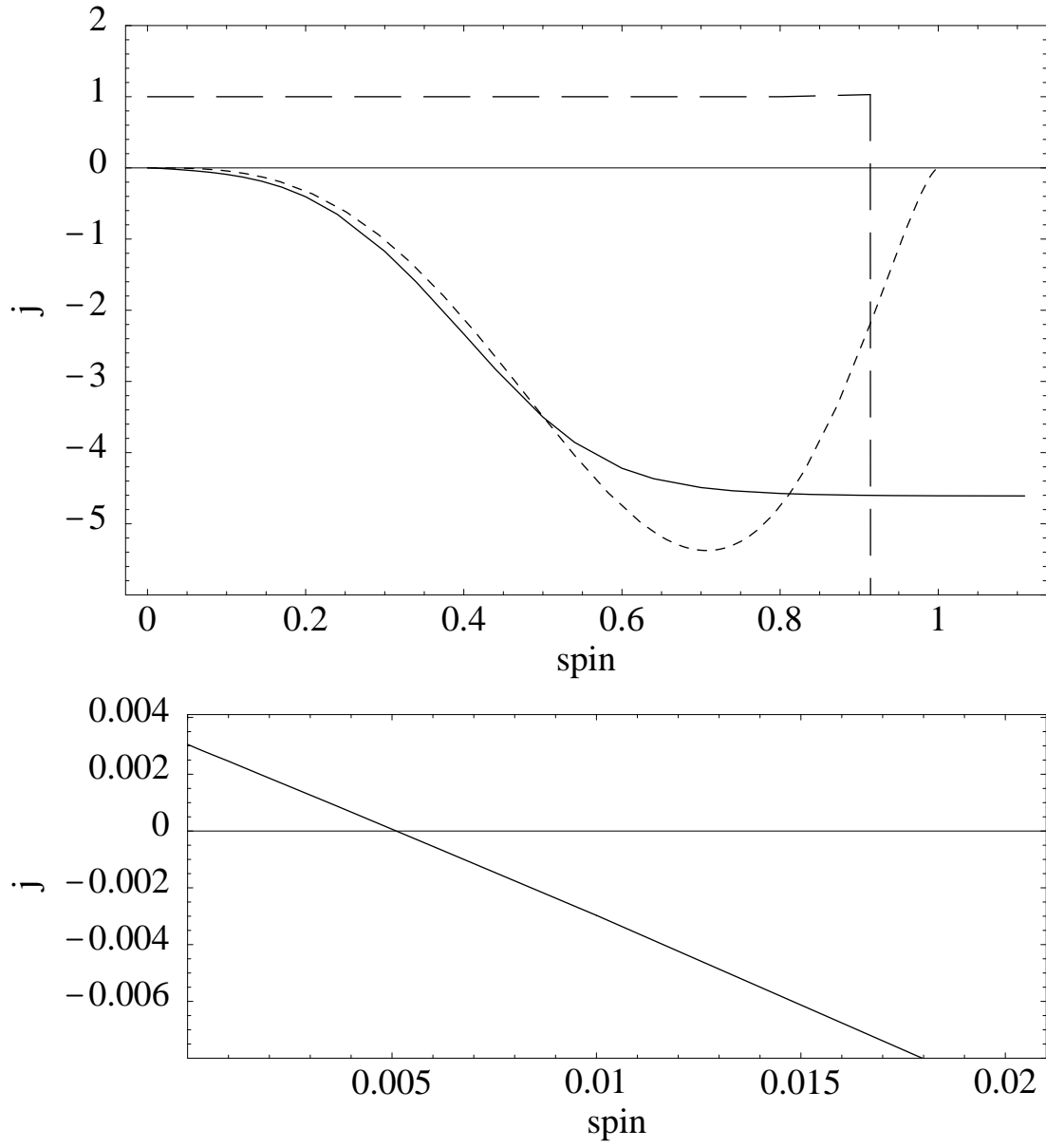


Fig.2

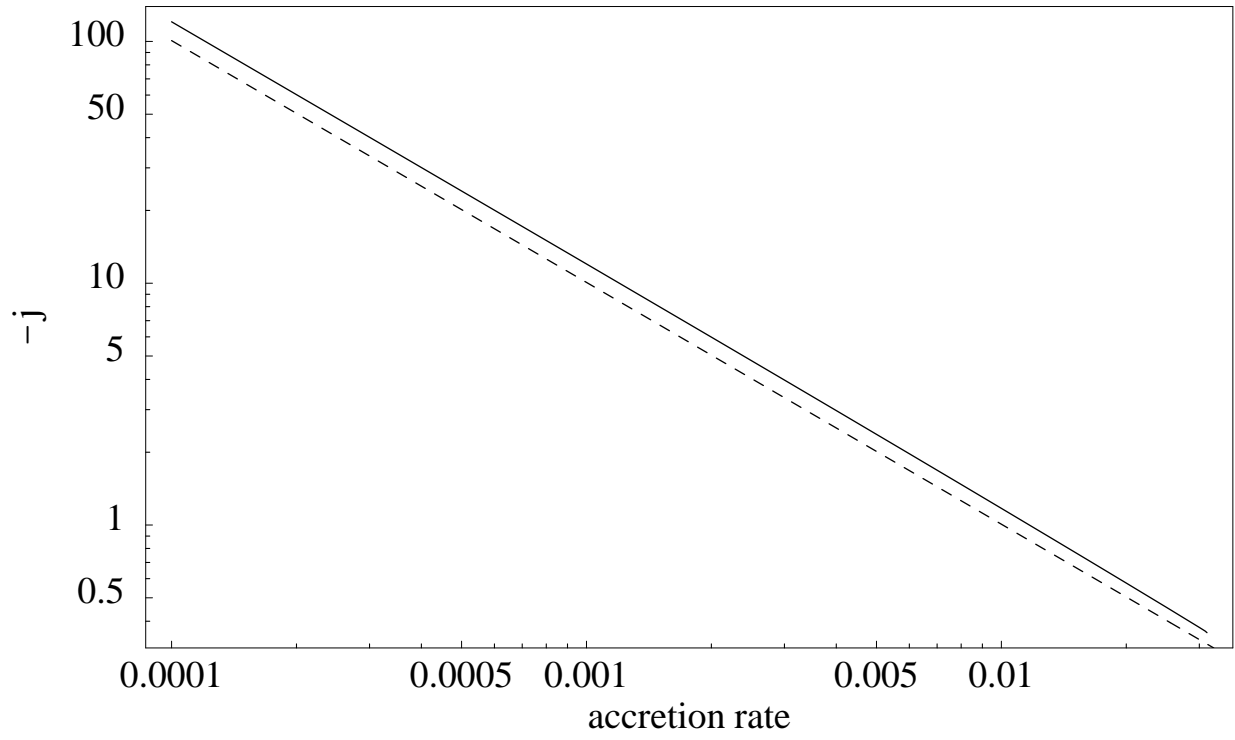


Fig. 3

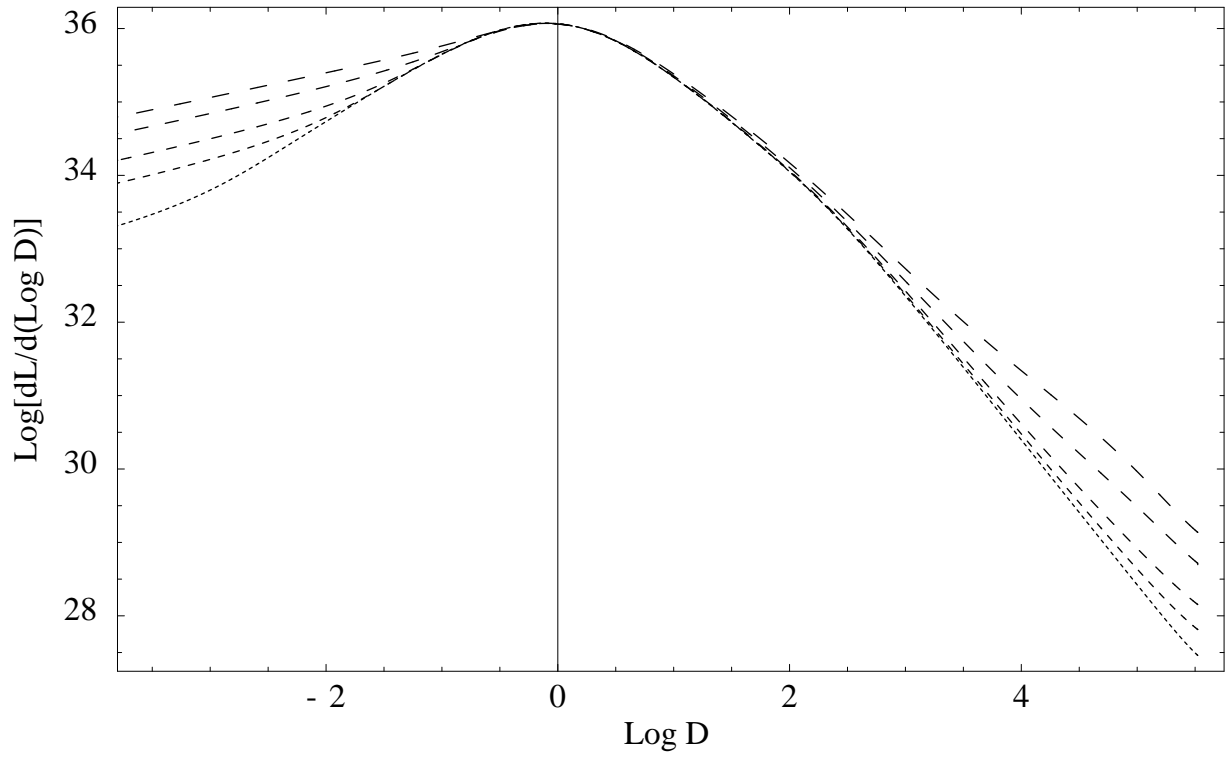


Fig.4

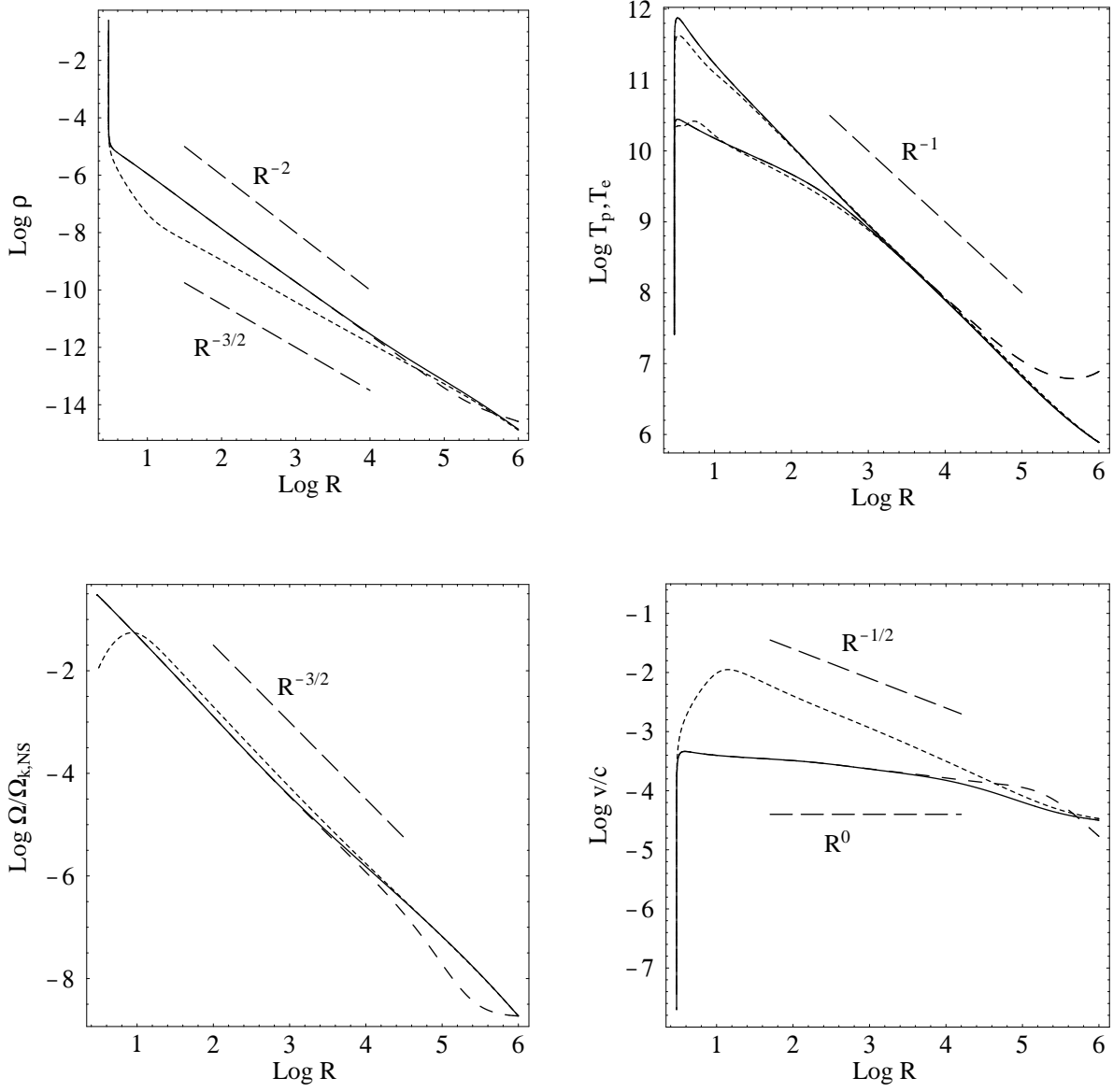


Fig. 5